JOURNAL OF APPLIED ELECTROCHEMISTRY 13 (1983) 135–145

A potentiodynamic study of anodic film formation on nickel in borate solutions

L. M. GASSA, J. R. VILCHE, A. J. ARVÍA

Instituto de Investigaciones Fisicoquímicas Teóricas y Aplicadas (INIFTA), División Electroquímica. Suc. 4, C.C. 16. (1900) La Plata, Argentina

Received 19 April 1982

The potentiodynamic behaviour of Ni in buffered borate electrolytes ($7.6 \leqslant pH \leqslant 9.3$) is investigated. The reactions taking place in the potential region of the $Ni/Ni(OH)_2$ and Ni(II)/Ni(III) redox couples can be formally interpreted with the same reaction patterns postulated for the electrochemical behaviour of nickel in strongly alkaline media including the multiplicity of phases related to the corresponding reactants and products. The main differences between the electrochemical characteristics of nickel over the whole pH range are in the growth rate of the anodic film and the change of its structure in relation to its degree of hydration, overall oxidation state and inner ionic composition.

1. Introduction

Anodic film formation on nickel has been extensively studied by means of electrochemical and optical methods covering a wide range of pH, solution composition, and temperature [1–3]. However, these studies are mainly focused either in the acid pH range emphasizing the passivation of nickel [1, 3–5] or in the alkaline electrolytes at pH greater than 12, because of the positive electrode reaction in the nickel alkaline battery [2, 3, 6, 7]. Comparatively, the literature on the electrochemical behaviour of nickel in neutral or slightly alkaline buffer solutions is more scarce [8–16]. The conclusions of various optical and electrochemical studies of nickel in neutral electrolytes agree that the film formation involves different oxidation states of nickel in two different potential ranges. The first passive layer is probably associated with $Ni(OH)_2$ formation which changes into a NiO layer reaching a limiting thickness of *ca.* 1.2 nm [15]. The amount of NiO film produced in neutral solution at a constant current depends, however, on the solution composition [11, 15, 16]. Thus, at the same pH, the film thickness is considerably thicker in borate than in sulphate electrolyte as in the latter the solubility of NiO is probably greater.

The anodic charging of nickel in borate solution at pH 7.65 in the potential range where the O_2 evolution begins, yields a fine porous oxide film which probably corresponds to the NiOOH-type species [16]. This suggests that a duplex structure thick film can be grown on nickel under galvanostatic conditions. The electrochemical response of the outer thick portion of the film is apparently similar to that observed for the Ni(II)/Ni(III) redox couple in alkaline solutions [5].

The purpose of the present work is to investigate the potentiodynamic response of nickel in the pH range from neutral to slightly alkaline solutions and to attempt to correlate its electrochemical behaviour over the whole potential range in terms of a single reaction pathway. Furthermore, the present results furnish information about multiplicity of species associated with the corresponding electrochemical reactions as it occurs both in strongly acid [3, 17, 18] and strongly alkaline [19, 20] electrolytes. This is in agreement with optical and photopotential data which indicate that in the neutral and slightly alkaline solutions multiplicity either of phases or states of reactants and products associated with the electrochemical reactions of nickel should also be considered [12, 14, 21, 22].

2. Experimental

The experimental set-up was as described in previous publications related to the electrochemical behaviour of nickel electrodes in acid [17, 18] and

0021–891X/83/020135–11$03.82/0

alkaline [19, 20] solutions. Specpure (Johnson Matthey Chem. Ltd.) polycrystalline nickel wires (0.5 mm diameter, 0.25 cm^2 apparent area) were employed. The potential of the working electrode was measured against a saturated calomel electrode located in a separate compartment connected through a fritted glass disc and cup-type glass stopcock lubricated with the same electrolytic solution, but in the text potentials are referred to the NHE scale. The following electrolyte solutions were used: 0.15 mol dm^{-3} $Na_2B_4O_7$ + z mol dm^{-3} H_3BO_3 (with $0.15 \leqslant z \leqslant 0.60$); and x mol dm^{-3} NaOH + y mol dm^{-3} Na_2SO_4 (with $10^{-3} \leqslant x \leqslant 1$, and $0 \leqslant y \leqslant 0.67$). They were prepared from thrice distilled water and analytical grade (p.a. Merck) reagents.

Experiments were performed under purified N_2 gas saturation at 25° C using: (a) single (STPS) and repetitive (RTPS) triangular potential scans between preset cathodic ($E_{s,c}$) and anodic ($E_{s,a}$) switching potentials, (b) single and repetitive galvanostatic pulses and step perturbations, (c) triangularly modulated triangular potential sweeps (TMTPS) and (d) complex combined potential perturbation programmes. The latter were employed to study the potentiodynamic, potentiostatic, and open circuit ageing of the electrochemically formed surface species.

Unless specifically stated the following description of results basically refers to runs made with borate–boric acid solution pH 9.3. Borate–boric acid solutions with decreasing pH values down to pH 7.6 were used to evaluate a possible pH dependence of the kinetic parameters in the 7.6 to 9.3 pH range. For the sake of comparison measurements in solutions containing sodium sulphate and in strong alkaline solutions were also made [19, 23].

3. Results

3.1. *The overall potentiodynamic E/I profile*

The RTPS E/I profile run between − 0.76 V– 1.24 V after previous cathodization at − 1.0 V (Fig. 1) shows in the first positive potential going scan the broad anodic current peak at *ca.* − 0.2 V (peak I) which corresponds to the $Ni(OH)_2$ formation and, in the potential range between *ca.* 0.8 V and 1.2 V, the current peaks (peaks II, III and IV) related to the complex redox system $Ni(OH)_2 \rightleftarrows NiOOH + H^+ + e$.

During the RTPS the height of peak I gradually decreases but the shapes of the complex peaks II and III remain practically unchanged although the corresponding charges increase. Peak IV appears more poorly defined as the pH decreases. Therefore, the potentiodynamic E/I response of nickel

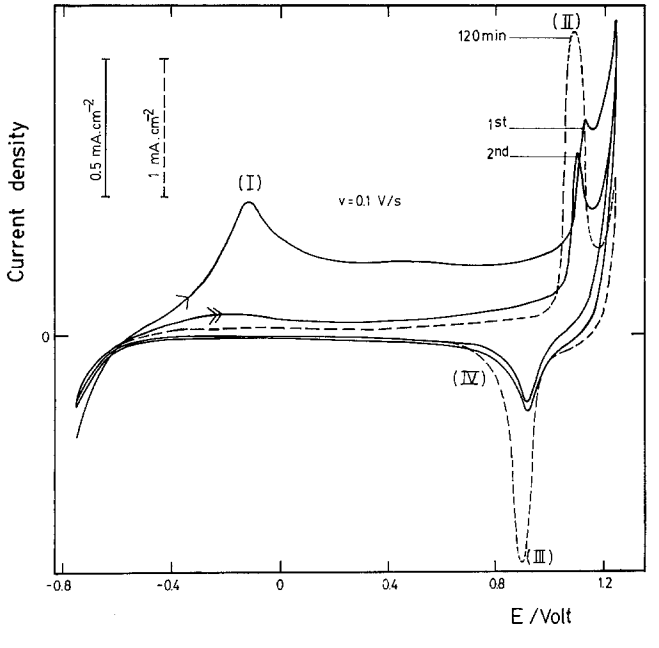

Fig. 1. Potentiodynamic displays obtained under RTPS at $v = 0.1$ V s^{-1} after a previous cathodization at − 1.0 V during 10 min. The first, the second and the E/I profile after 120 min cycling are shown; pH 9.3.

in buffered solutions ($7.6 \leqslant pH \leqslant 9.3$) in the potential range of $Ni(OH)_2$ formation is, in principle, similar to that already known in strong alkaline solutions ($pH > 12$) [19, 24–26].

3.2. *The E/I profile related to the Ni/Ni(OH)$_2$ electrode*

The charge involved in current peak I during the first anodic potential going excursion is relatively low. If one assumes for the electrode a roughness factor of about 2, the $Ni(OH)_2$ charge can be assigned to the formation of a $Ni(OH)_2$ monolayer. The dependence of the height of peak I ($i_{p,I}$) and the corresponding peak potential ($E_{p,I}$) on potential scan rate, v, and on pH (in the pH range $7 < pH < 14$) are given by the following relationships (Figs. 2–4):

$$(\partial E_{p,I}/\partial \log v)_{pH} = 0.064 \pm 0.007 \text{ V decade}^{-1}$$

$$(\partial \log i_{p,I}/\partial \log v)_{pH} = 0.95 \pm 0.10$$

$$(\partial \log i_{p,I}/\partial \text{ pH})_v = 0 \pm 0.05$$

$$(\partial E_{p,I}/\partial \text{ pH})_v = -0.068 \pm 0.007 \text{ V decade}^{-1}.$$

A systematic study of the E/I profiles in the $Ni(OH)_2$ formation potential range shows that peak I exhibits complementary cathodic current peak (peak V) at *ca.* -0.62 V which partially overlaps the hydrogen evolution current (Figs. 5 and 6). The potentiodynamic E/I profiles, run with a STPS at a preset v starting from different values of $E_{s,c}$ after a constant cathodic polarization time at this potential, show the height of peak I depends on $E_{s,c}$ when $E_{s,c} > -0.8$ V, but is independent of it when $E_{s,c} < -0.95$ V (Fig. 5a). Furthermore, the height of peak V ($i_{p,V}$) and the corresponding peak potential ($E_{p,V}$) depend on the $E_{s,a}$ value. The degree of reversibility of the redox couple associated with peaks I and V can be, in principle, correlated to the peak potential difference $\Delta E_p = E_{p,I} - E_{p,V}$ · ΔE_p decreases as v decreases (Fig. 5). Unfortunately the extrapolation of ΔE_p to $v \to 0$ is not feasible due to the overlapping of peak V with the E/I profile of the hydrogen evolution reaction (Fig. 5b).

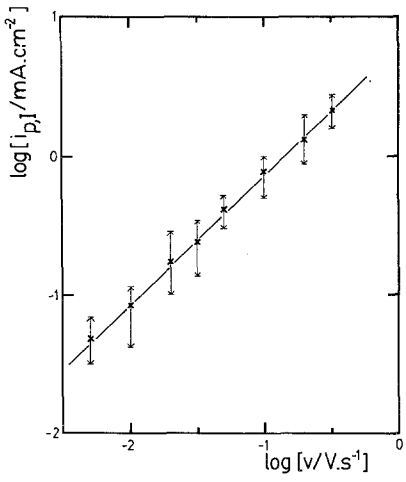

Fig. 3. Dependence of $i_{p,I}$ on v from STPS employing electrolytic solutions with pH values ranging between 7.6 and 13.9. Both the mean $i_{p,I}$ and the limiting $i_{p,I}$ values for all solutions pH at each v are indicated.

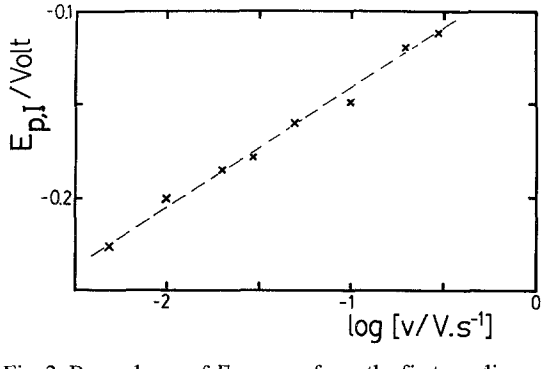

Fig. 2. Dependence of $E_{p,I}$ on v from the first anodic potential scan; borate–boric solution, pH 9.3.

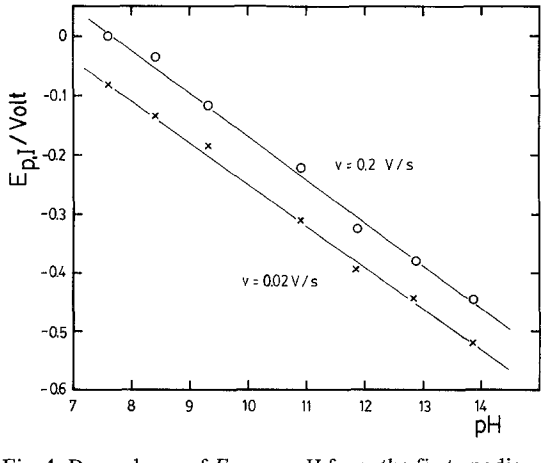

Fig. 4. Dependence of $E_{p,I}$ on pH from the first anodic potential excursions. (×) $v = 0.02$ V s^{-1}; (○) $v = 0.2$ V s^{-1}.

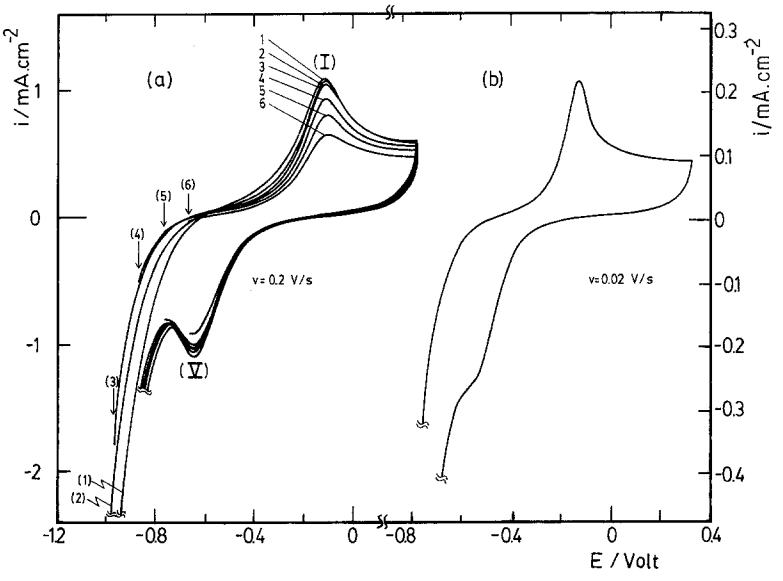

Fig. 5. Potentiodynamic E/I contours obtained under STPS. (a) Influence of $E_{s,c}$ on the E/I curves recorded as 0.2 V s^{-1}: (1) $E_{s,c} = -1.2$ V; (2) $E_{s,c} = -1.1$ V; (3) $E_{s,c} = -1.0$ V; (4) $E_{s,c} = -0.9$ V; (5) $E_{s,c} = -0.8$ V; and (6) $E_{s,c} = -0.7$ V. (b) STPS E/I profile run at 0.02 V s^{-1}, $E_{s,c} = -1.1$ V.

RTPS runs within the potential range of the $Ni/Ni(OH)_2$ electrode show a stabilized E/I profile after 3–5 min potential cycling. The anodic portion of the voltammogram recorded at the nth cycle in comparison with that of the first cycle is slightly shifted towards negative potentials (Fig. 6). The E/I characteristics obtained in borate solutions ($7.6 \leqslant pH \leqslant 9.3$) exhibit the same features. At pH 7.6 the stabilized E/I contours run at different values of v (Fig. 7) show a remarkable symmetry of peaks I and V once both the baseline corrections for the passivity current and the hydrogen discharge current were taken into account. At the nth potential cycle both $i_{p,I}$ and $i_{p,V}$ change linearly with v.

The shapes of current peaks I and V are very sensitive to $E_{s,a}$ (Fig. 8). Thus, as $E_{s,a}$ becomes more positive it appears that the oxide–hydroxide layer is hardly electroreducible. In this case the electrode passivity increases progressively as $E_{s,a}$ becomes more positive. Then, peaks I and V are no longer distinguishable. On the other hand, the initial reactivity of the electrode is recovered after cathodizing at $E_{s,c}$ values about -0.8 to -0.9 V. Nevertheless, when the cathodization proceeds at $E_{s,c} < -1.1$ V, during a relatively long time, then an anodic current pre-peak is observed in the potential range preceding peak I. The location of this peak, however, depends both on the cathodization potential and on v. Furthermore, at very low v ($v < 0.002$ V s^{-1}) a new anodic shoulder appears at potentials more positive than that of peak I. This is similar to the anodic contribution observed at higher v in acid solutions within the active–passive transition potential range [17, 18].

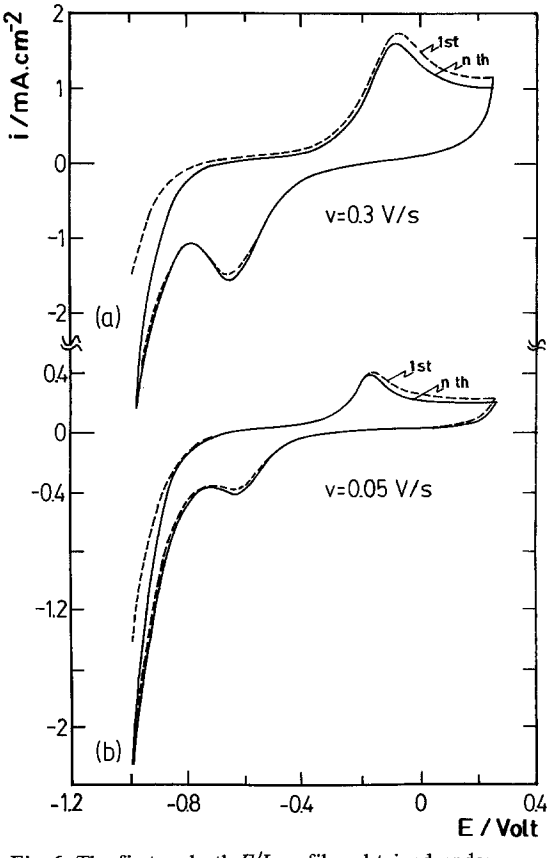

Fig. 6. The first and nth E/I profiles obtained under RTPS. (a) $v = 0.3$ V s^{-1}; (b) $v = 0.05$ V s^{-1}.

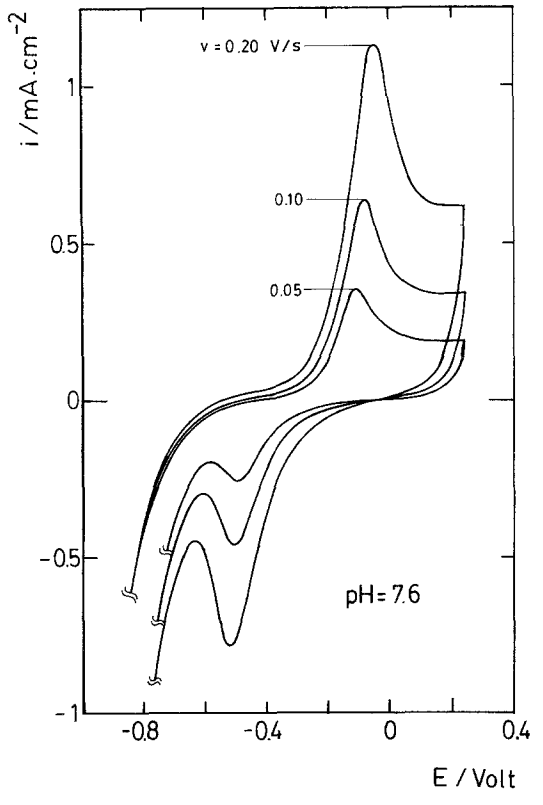

Fig. 7. Stabilized RTPS *E/I* profiles run at different values of v between $E_{s,c} = -1.16$ V and $E_{s,a} = 0.24$ V; pH 7.6.

3.3. *The E/I profile related to the potential range of Ni(II)/Ni(III)*

The RTPS *E/I* profile obtained in borate buffers ($7.6 \leqslant pH \leqslant 9.3$) in the potential range of the Ni(II)/Ni(III) couple (Figs. 9 and 10) is, in principle, similar to that already observed in strong alkaline electrolytes [19, 20]. Although in strong alkaline solutions peak III is much thinner than peak II a situation which is reversed in slightly alkaline and neutral electrolytes. The charges involved both in the anodic and cathodic reactions are equal, in the order of 1.45 mC cm^{-2} apparent area at $v = 0.2$ V. For comparable runs the potentials of the different current peaks shift linearly with the solution pH (Fig. 11). The increase in $\Delta E'_p$ ($\Delta E'_p = E_{p,II} - E_{p,III}$) as the pH decreases (Fig. 11) is probably due to the fact that only small v values are required in solutions approaching neutrality to achieve the independence of peak potential values on solution pH (Fig. 12), while at pH 14 both $E_{p,II}$ and $E_{p,III}$ values remain practically independent of v at least for $v < 0.03$ V s^{-1} [19]. The height of peak II ($i_{p,II}$) fits a linear dependence on v, which coincides with that found in 1 mol dm^{-3} KOH (Fig. 13). From these results one concludes $(\partial \log i_{p,II}/\partial\, pH)_v \approx 0$.

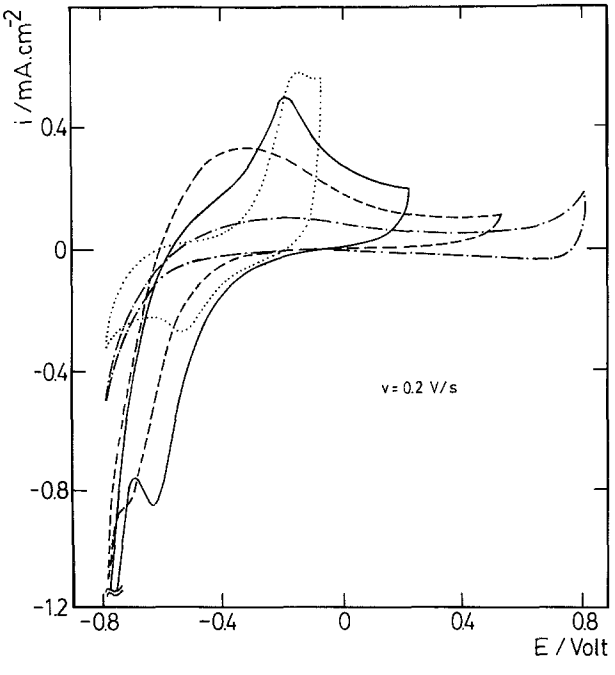

Fig. 8. Influence of $E_{s,a}$ on the stabilized RTPS *E/I* displays recorded at 0.2 V s^{-1}.

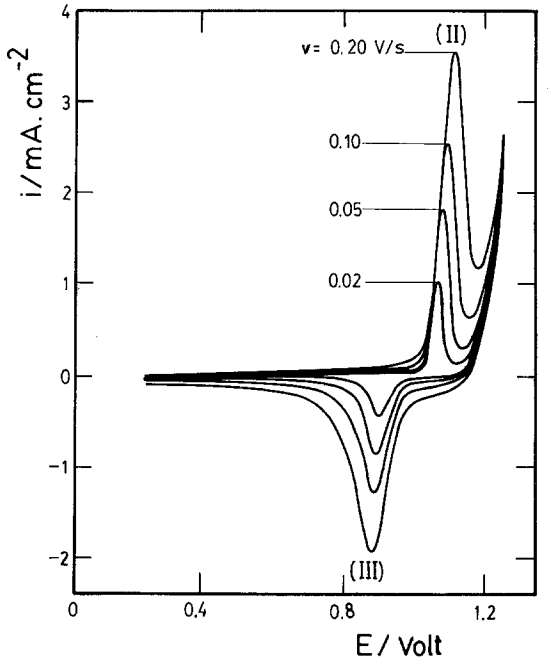

Fig. 9. Stabilized RTPS *E/I* displays run at different values of v; pH 9.3.

The *E/I* contours recorded with asymmetric RTPS, either with a constant v_a and a variable v_c (Fig. 14a) or vice versa (Fig. 14b), exhibit a wide cathodic peak (peak III) and a relatively sharp anodic peak (peak II), the increasing portions of the latter being coincident and approaching a straightline relationship.

The complexity of peak II (Fig. 15) is evident when applying to the electrode the perturbation programme depicted in the figure. As the time τ corresponding to the intermediate perturbation between $E'_{s,a}$ and $E_{s,c}$ increases, the charge related to the peak located at 1.10 V decreases and correspondingly, that of the peak at 1.15 V increases. This effect is also similar to that earlier described for KOH aqueous solutions [20, 27]. An analogous splitting is achieved in the electroreduction profile by properly selecting $E'_{s,c}$ and τ (Fig. 16) [19, 25]. The periodic potential perturbation including a potential holding at $E_{s,a}$ yields an accumulation of product which electroreduces at potentials more negative than the potential of peak III (Fig. 17). In this case the inclusion of a potential holding at $E_{s,a}$ implies an enhancement of the electroreduction charge and an increase in the height of the current peak IV, (Fig. 17a) but when the holding at the potential $E_{s,a}$ is interrupted, then the *E/I* profile comes back to the conventional stabilized RTPS *E/I* profile (Fig. 17b).

There is a remarkable influence of $E_{s,c}$ on the *E/I* profile in the potential range of current peak II. Thus, as $E_{s,c}$ becomes more positive (Fig. 18)

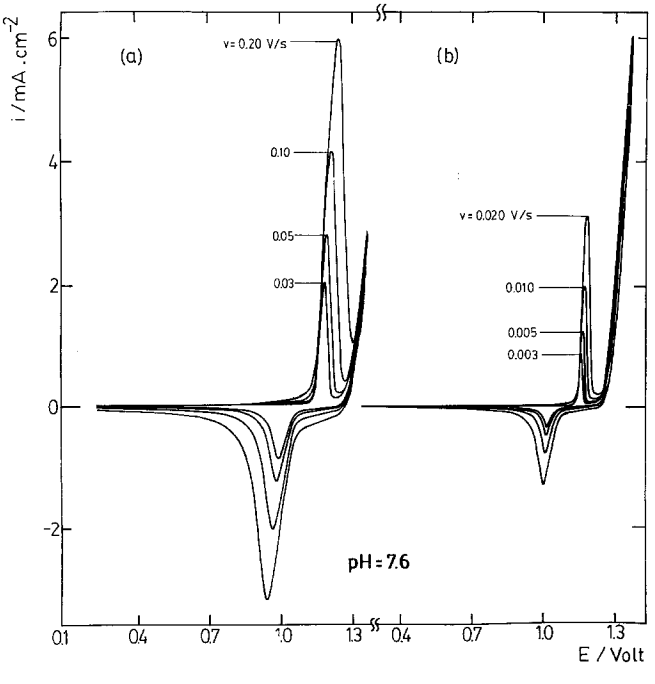

Fig. 10. Stabilized RTPS *E/I* displays run at different values of v; pH 7.6.

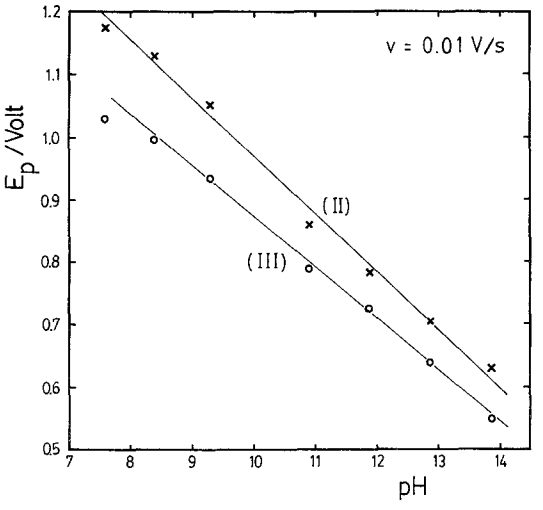

Fig. 11. Dependence of $E_{p,II}$ (×) and $E_{p,III}$ (○) on pH measured with RTPS at 0.01 V s^{-1} employing comparable switching potentials.

the anodic process begins gradually at lower potentials. It appears that the relative amount of the Ni(III) surface species which remains on the electrode at $E_{s,c}$ diminishes, and accordingly some polarization contributes during the anodic process. The effect is similar to that observed through the TMTPS experiments reported in strong alkaline solutions [28]. However, as $E_{s,c}$ is extended towards negative values, the complete electroreduction of the Ni(III) containing film is achieved.

3.4. *Galvanostatic runs*

The potential response to both anodic and cathodic current steps (Figs. 19 and 20) shows clear transition times in the potential range of both the $Ni(OH)_2$ electrode and the Ni(II)/Ni(III) redox couple. The definition on the transition times depends remarkably on the duration of the potential step. They reveal the occurrence of one main process in the potential range of the $Ni(OH)_2$ electrode and the occurrence of at least two processes in the potential range of the Ni(II)/Ni(III) redox couple.

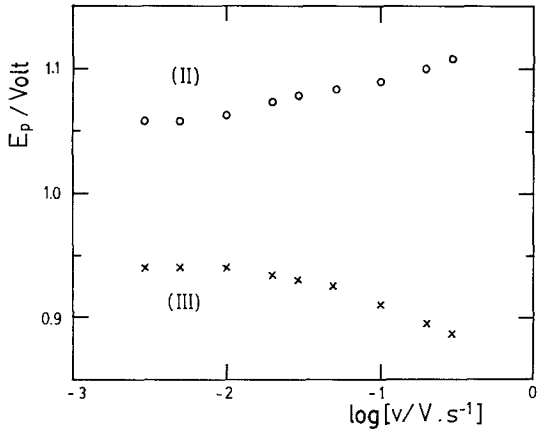

Fig. 12. Dependence of $E_{p,II}$ (○) and $E_{p,III}$ (×) on v measured in borate–boric acid solution; pH 9.3.

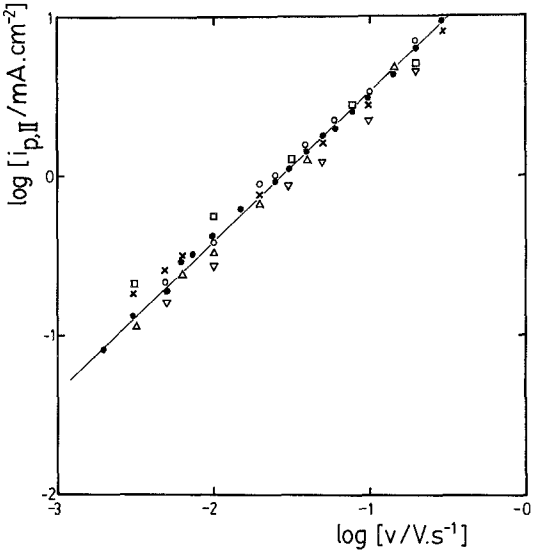

Fig. 13. Dependence of $i_{p,II}$ on v from RTPS. Borate–boric acid solutions: (×) pH 9.3; (▽) pH 8.4; (□) pH 7.6. KOH + K_2SO_4 solutions: (△) pH 11.9; (○) pH 12.9; (●) pH 13.8. The full line corresponds to the measurements run using 1 mol dm^{-3} KOH.

4. Discussion

There is apparently a similar potentiodynamic behaviour of nickel in strong alkaline electrolyte and in electrolytes approaching neutrality. The behaviour of nickel in buffered borate solutions ($7.6 \leqslant pH \leqslant 9.3$) exhibits at low potentials the response related to the $Ni + H_2O = Ni(OH)_2 + 2H^+ + 2e$ reaction and at high positive potentials that of the formation of Ni(III) species, according to the reaction: $Ni(OH)_2 \rightleftharpoons NiOOH + H^+ + e$. The characteristics of the former process is to some extent similar to that found in sulphate containing solutions in the acid pH range. In this case, the product initially formed undergoes a series of chemical and electrochemical transformations which can be derived from the E/I profile resulting

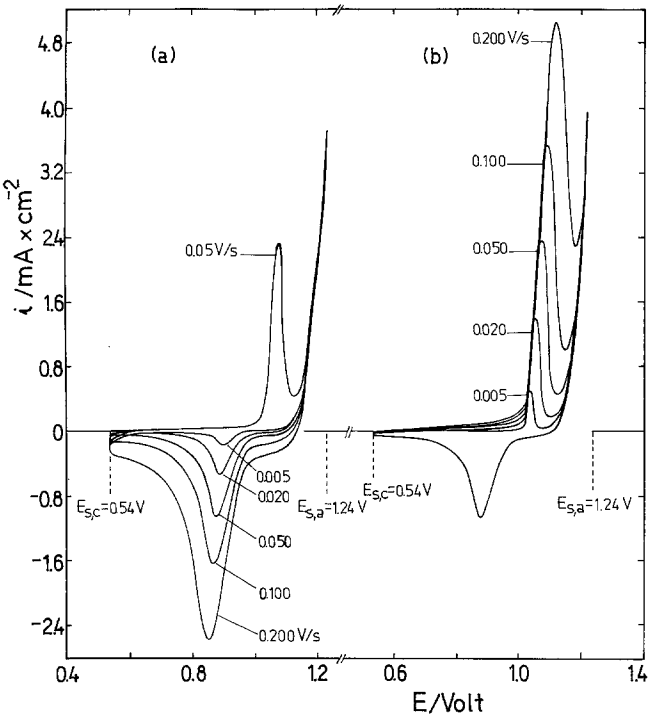

Fig. 14. Potentiodynamic *E/I* displays run under asymmetric RTPS conditions. (a) $v_a = 0.05\ V\ s^{-1}$ and different v_c; (b) $v_c = 0.05\ V\ s^{-1}$ and different v_a.

from a systematic combination and change of the potential perturbation condition. The final product which is related to the passive oxide film is NiO [15–18]. Within the 5.5 to 9.5 pH range the thickness of the latter is practically independent of the solution pH and on the type of anions in solutions [14]. Unlike the NiO passive film formed under potentiostatic conditions at high potentials, the oxo-hydroxide film produced under potentiodynamic conditions in the range pH 7.6–9.3 is believed to be associated with its electroreduction to $Ni(OH)_2$ in an overall conversion reaction probably similar to that proposed for charging and discharging the nickel alkaline battery [2, 3, 6, 7]. In this case the multiplicity of phases found for both reactions taking place in the potential range of both the $Ni(OH)_2$ electrode and the Ni(II)/Ni(III) redox couple by means of the potentiodynamic perturbation techniques adds considerably to the complications of using simple kinetic models for interpreting optical data [12].

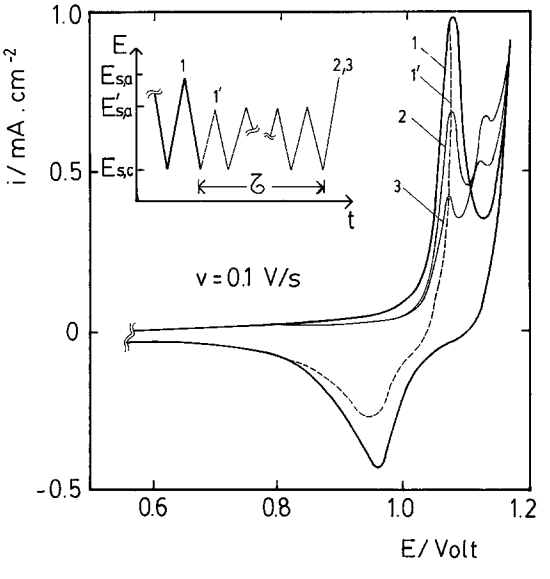

Fig. 15. Potentiodynamic *E/I* displays obtained with the perturbation programme depicted in the figure. $E_{s,c} = 0.240\ V$, $E_{s,a} = 1.17\ V$, $E'_{s,a} = 1.06\ V$, $v = 0.1\ V\ s^{-1}$. (1) Influence of τ on the stabilized RTPS *E/I* contour. (2) $\tau = 10$ min; (3) $\tau = 15$ min.

In the Ni(II)/Ni(III) redox couple potential range a structural change of the passivating thin layer in the vicinity of the equilibrium potential of the oxygen electrode furnishes catalytic properties for the oxygen evolution reaction [29]. The time dependence of the photopotential which was explained by a doping mechanism which changes p-type oxide into the n-type oxide, correlates with the multiplicity of states found in the buffered borate solutions.

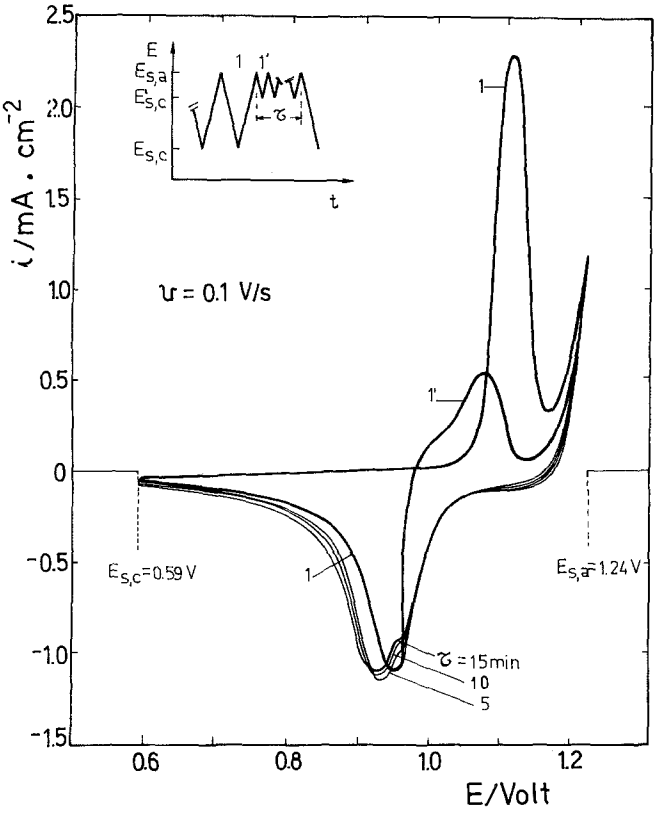

Fig. 16. Complex potentiodynamic E/I contours obtained with the perturbation programme depicted in the figure.

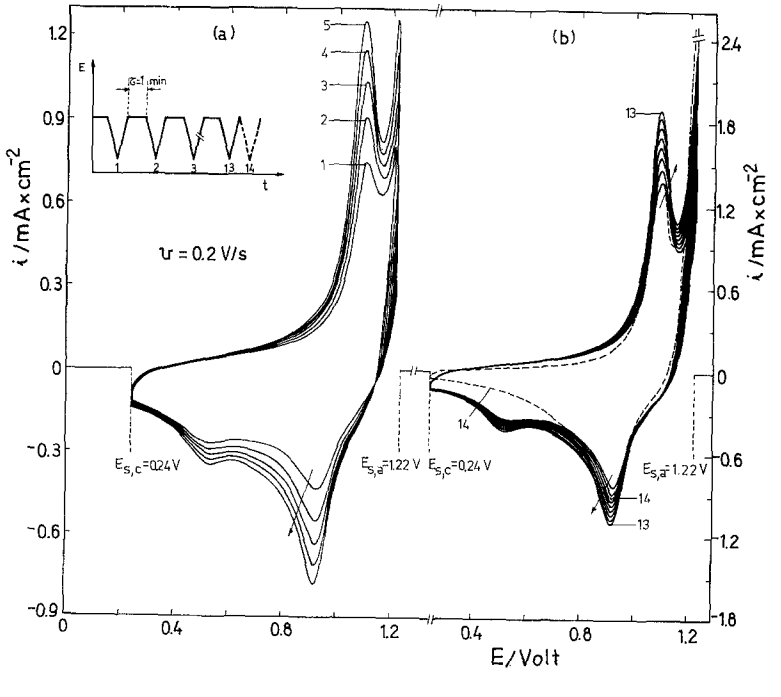

Fig. 17. Potentiodynamic E/I curves recorded after including a potential holding at $E_{s,a}$ during 1 min. The dotted line shows the E/I profile obtained at the 14th cycle without holding the potential at $E_{s,a}$.

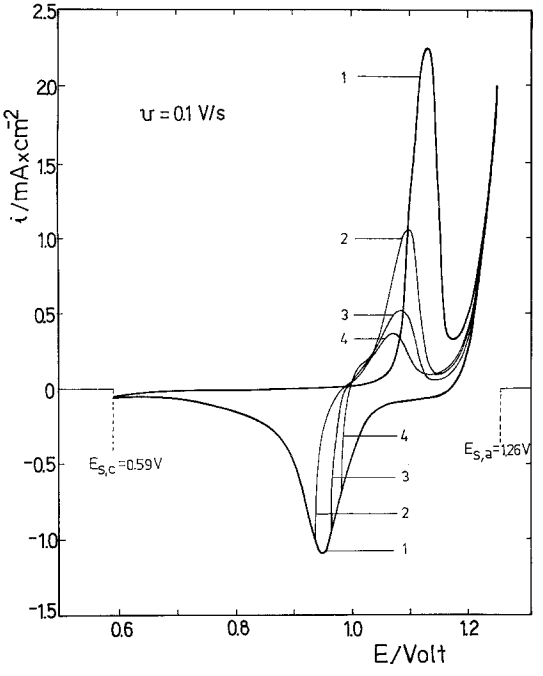

Fig. 18. Influence of $E_{s,c}$ on the E/I profiles recorded with RTPS at 0.1 V s^{-1}.

The kinetic parameters related to peak I in the weak alkaline buffered electrodes are analogous to those previously reported in strong alkaline solutions [23] and also comparable to those earlier reported for acid electrolytes [18] if one takes into account that in the former case there

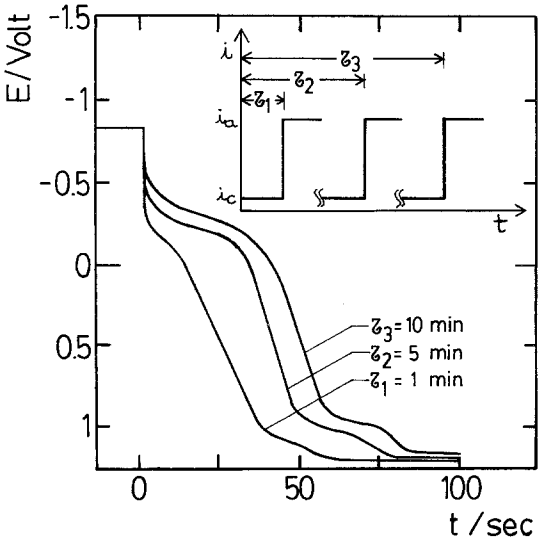

Fig. 19. Galvanostatic charging curves at $i_a = 108\ \mu A\ cm^{-2}$ after different holding times at $i_c = -64\ \mu A\ cm^{-2}$ in the hydrogen evolution potential region; pH 9.3.

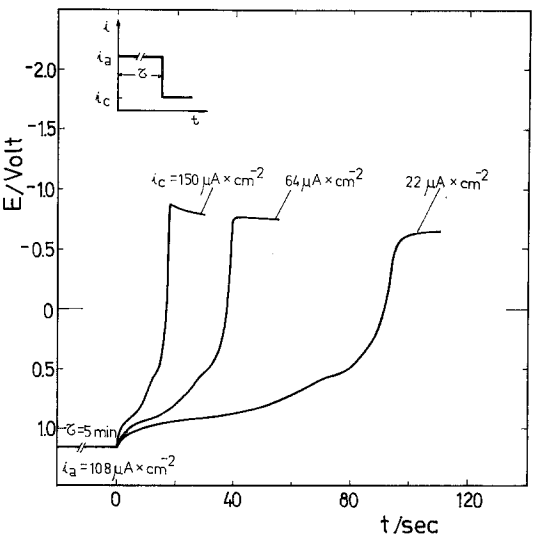

Fig. 20. Galvanostatic discharging curves at different i_c after 5 min anodization at $i_a = 108\ \mu A\ cm^{-2}$; pH 9.3.

is no chemical dissolution of the $Ni(OH)_2$ film. This means that as the pH increases the mechanism of the potentiodynamic formation of the $Ni(OH)_2$ layer changes from a predominantly precipitation–dissolution mechanism at low pH [$(\partial E_{p,I}/\partial \log v) = 0.062$ and $(\partial \log i_{p,I}/\partial \log v) = 0.5$] to an activation-controlled film-forming mechanism at high pH [$(\partial E_{p,I}/\partial \log v)_{pH} = 0.064$ and $(\partial \log i_{p,I}/\partial \log v)_{pH} \simeq 1.0$)]. There is therefore, a continuity in the validity of the reaction pattern for the behaviour of $Ni/Ni(OH)_2$ electrode in aqueous electrolytes including those containing either sulphate or borate ions in going from the strong alkaline to the acid solutions. The overall process consists then of the solvent-assisted metal electro-oxidation yielding hydroxo-containing species and the deprotonation of the latter in successive steps including between the first and the second electron transfer step, a chemical change to the surface film [23]. On the assumption that a uniform $Ni(OH)_2$ layer is formed the kinetic data can be formally accounted for when the chemical process is the rate determining step.

The main difference between the electrochemical behaviour of nickel in strongly alkaline and weakly alkaline solutions is found in the growth rate of the anodic film. As recently reported for the galvanostatic oxidation of nickel in borate buffer solutions [16, 30], the stability of the passive films both towards open circuit break-

down and electroreduction depends strongly on both the time and the potential of anodic film treatment.

The present results confirm that in borate electrolyte, thicker oxide films can be grown at potentials in the oxygen evolution potential region and are coincident with the fact that films formed in the passivation of nickel in phosphate containing solutions exhibit the same optical constants at pH 9.1 and 4.5 but different growth rates [14]. The increase in thickness of the anodic film at anodic potentials after prolonged polarization occurs through additional film formation on top of the passive film. In this case, the composition changes, so that as the potential increases the film is probably partially dehydrated [30–32] and decreases in thickness. The charges involved in the potentiodynamic *E/I* profiles confirm that a secondary passivation occurs in the oxygen evolution potential region, a fact which correlates with the abrupt increase in the optical constants of the film which depend on its thickness [33]. In this case Ni^{2+} ions should go into solution only after the passivation film grows to its steady state thickness. Then, in addition to the chemical or electrochemical dissolution of the film, a mechanism involving a film breakdown which continuously produces microbreakdown sites should simultaneously operate. As recently pointed out [16] this mechanism of direct oxidation should correspond to a misorientation associated with the increase in the layer thickness, yielding an open cellular sponge-type film.

Acknowledgement

INIFTA is sponsored by Consejo Nacional de Investigaciones Científicas y Ténicas, the Universidad Nacional de La Plata and the Comisión de Investigaciones Científicas (Provincia de Buenos Aires).

References

[1] V. Brusic, 'Oxides and Oxide Films', Vol. 1 (edited by J. W. Diggle) Marcel Dekker, New York (1972) p. 1.
[2] G. W. D. Briggs, 'Electrochemistry', Vol. 4, Specialist Periodical Reports. The Chemical Society, London (1974) p. 33.
[3] A. J. Arvía and D. Posadas, 'The Electrochemistry of the Elements', Vol. 3 (edited by A. J. Bard) Marcel Dekker, New York (1975) p. 212.
[4] J. L. Ord, in 'Passivity of Metals' (edited by R. P. Frankenthal and J. Kruger), The Electrochemical Society Inc., Princeton (1978) p. 273.
[5] J. R. Vilche and A. J. Arvía, in *idem.*, p. 861.
[6] P. C. Milner and U. B. Thomas, in 'Advances in Electrochemistry and Electrochemical Engineering', Vol. 5 (edited by C. W. Tobias) Interscience, New York (1967) p. 1.
[7] S. U. Falk and A. J. Salkind, 'Alkaline Storage Batteries', John Wiley & Sons, New York (1969).
[8] S. Lipanovic and B. Lovrecek, *Corros. Sci.* **12** (1972) 637.
[9] M. Okuyama and S. Haruyama, *Corros. Sci.* **14** (1974) 1.
[10] N. Sato and K. Kudo, *Electrochim. Acta* **19** (1974) 461.
[11] B. MacDougall and M. Cohen, *J. Electrochem. Soc.* **121** (1974) 1152.
[12] J. L. Ord, J. C. Clayton and D. J. DeSmet, *J. Electrochem. Soc.* **124** (1977) 1714.
[13] O. G. Deryagina and E. N. Paleolog, *Elektrokhimiya* **14** (1978) 996.
[14] C. Y. Chao and Z. Szklarka-Smialowska, *Surface Sci.* **96** (1980) 426.
[15] B. MacDougall, D. F. Mitchell and M. J. Graham, *J. Electrochem. Soc.* **127** (1980) 1248.
[16] B. MacDougall and M. J. Graham, *J. Electrochem. Soc.* **128** (1981) 2321.
[17] J. R. Vilche and A. J. Arvía, *Corros. Sci.* **18** (1978) 441.
[18] S. G. Real, J. R. Vilche and A. J. Arvía, *ibid.* **20** (1980) 563.
[19] R. S. Schrebler Guzmán, J. R. Vilche and A. J. Arvía, *J. Electrochem. Soc.* **125** (1978) 1578.
[20] H. Gomez Meier, J. R. Vilche and A. J. Arvía, *J. Appl. Electrochem.* **10** (1980) 611.
[21] W. Paatsche, *Surface Sci.* **37** (1973) 59.
[22] W. Paatsche, *Proc. 7th Int. Congr. Met. Corros.*, Río de Janeiro (1978) p. 213.
[23] R. S. Schrebler Guzmán, J. R. Vilche and A. J. Arvía, *Corros. Sci.* **18** (1978) 765.
[24] J. R. Vilche and A. J. Arvía, *Proc. 1st Symp. Bras. Electrochim. Electroanal.*, Sao Paulo (1978) p. 85.
[25] R. S. Schrebler Guzmán, J. R. Vilche and A. J. Arvía, *J. Appl. Electrochem.* **8** (1978) 69.
[26] J. R. Vilche and A. J. Arvía, *Proc. 7th Int. Congr. Met. Corros.*, Río de Janeiro (1978) p. 245.
[27] R. S. Schrebler Guzmán, J. R. Vilche and A. J. Arvía, *J. Appl. Electrochem.* **9** (1979) 183.
[28] *Idem, ibid.* **9** (1979) 321.
[29] C. R. Davidson and S. Srinivasan, *J. Electrochem. Soc.* **127** (1980) 1060.
[30] L. M. Gassa, J. R. Vilche and A. J. Arvía, *Proc. 5th Lat. Am. Meet. Electrochem. Corros.*, Concepción (1980) p. 179.
[31] M. E. Folquer, J. R. Vilche and A. J. Arvía, *J. Electrochem. Soc.* **127** (1980) 2634.
[32] V. A. Macagno, J. R. Vilche and A. J. Arvía, *ibid.* **129** (1982) 301.
[33] N. Sato, K. Kudo and M. Miki, *J. Chem. Soc. Japan* **10** (1971) 1007.